Sodium temperature lidar based on injection seeded Nd:YAG pulse lasers using a sum-frequency generation technique

Takuya D. Kawahara,[1,*] Tsukasa Kitahara,[1,2] Fumitoshi Kobayashi,[1] Yasunori Saito,[1] and Akio Nomura[3]

[1]*Faculty of Engineering, Shinshu University, 4-17-1 Wakasato, Nagano-shi, 380-8553, Japan*
[2]*Currently with Toba National College of Maritime Technology, 1-1 Ikegami, Toba-shi, Mie, 517-8501, Japan*
[3]*Formerly with Faculty of Engineering, Shinshu University, 4-17-1 Wakasato, Nagano-shi, 380-8553, Japan*
**kawahara@cs.shinshu-u.ac.jp*

Abstract: We report on a sodium (Na) temperature lidar based on two injection seeded Nd:YAG pulse lasers using single-pass sum-frequency generation. The laser power at 589 nm is 400 mW (40 mJ per pulse at a repetition rate of 10 Hz) and the pulse width is 22 nsec FWHM. The narrowband laser tuned to the Doppler broadened Na D_2 spectrum enables us to measure the temperature of the mesopause region (80-115 km). This solid-state transportable system demonstrated high performance and capability at Syowa Station in Antarctica for 3 years and at Uji in Japan for an additional year without any major operational troubles.

OCIS codes: (140.3580) Lasers, solid-state; (280.3640) Lidar; (280.6780) Temperature; (010.0280) Remote sensing and sensors.

References and links

1. C.-Y. She, and J. R. Yu, "Simultaneous three-frequency Na lidar measurements of radial wind and temperature in the mesopause region," Geophys. Res. Lett. **21**(17), 1771–1774 (1994).
2. U. von Zahn, and J. Höffner, "Mesopause temperature profiling by potassium lidar," Geophys. Res. Lett. **23**(2), 141–144 (1996).
3. J. S. Friedman, C. A. Tepley, S. Raizada, Q. H. Zhou, J. Hedin, and R. Delgado, "Potassium Doppler-resonance lidar for the study of the mesosphere and lower thermosphere at the Arecibo Observatory," J. Atmos. Sol. Terr. Phys. **65**(16-18), 1411–1424 (2003).
4. X. Chu, W. Pan, G. C. Papen, C. S. Gardner, and J. A. Gelbwachs, "Fe Boltzmann temperature lidar: design, error analysis, and initial results at the north and south poles," Appl. Opt. **41**(21), 4400–4410 (2002).
5. C. S. Gardner, "Performance Capabilities of Middle-Atmosphere Temperature Lidars: Comparison of Na, Fe, K, Ca, Ca^+, and Rayleigh Systems," Appl. Opt. **43**(25), 4941–4956 (2004).
6. T. H. Jeys, A. A. Brailove, and A. Mooradian, "Sum frequency generation of sodium resonance radiation," Appl. Opt. **28**(13), 2588–2591 (1989).
7. T. Nishikawa, A. Ozawa, Y. Nishida, M. Asobe, F.-L. Hong, and T. W. Hänsch, "Efficient 494 mW sum-frequency generation of sodium resonance radiation at 589 nm by using a periodically poled Zn:LiNbO3 ridge waveguide," Opt. Express **17**(20), 17792–17800 (2009).
8. N. Saito, K. Akagawa, M. Ito, A. Takazawa, Y. Hayano, Y. Saito, M. Ito, H. Takami, M. Iye, and S. Wada, "Sodium D_2 resonance radiation in single-pass sum-frequency generation with actively mode-locked Nd:YAG lasers," Opt. Lett. **32**(14), 1965–1967 (2007).
9. T. D. Kawahara, T. Kitahara, F. Kobayashi, Y. Saito, A. Nomura, C.-Y. She, D. A. Krueger, and M. Tsutsumi, ""Wintertime mesopause temperatures observed by lidar measurements over Syowa station (69°S, 39°E)," Antarctica," Geophys. Res. Lett. **29**(15), 1709 (2002), doi:10.1029/2002GL015244.
10. M. K. Ejiri, T. Nakamura, and T. D. Kawahara, "Seasonal variation of nocturnal temperature and sodium density in the mesopause region observed by a resonance scatter lidar over Uji, Japan," J. Geophys. Res. **115**(D18), D18126 (2010), doi:10.1029/2009JD013799.
11. R. E. Bills, C. S. Gardner, and C.-Y. She, "Narrowband lidar technique for sodium temperature and Doppler wind observations of the upper atmosphere," Opt. Eng. **30**(1), 13–21 (1991).
12. G. B. Burns, T. D. Kawahara, W. J. R. French, A. Nomura, and A. R. Klekociuk, "A comparison of hydroxyl rotational temperatures from Davis (69°S, 78°E) with sodium lidar temperatures from Syowa (69°S, 39°E)," Geophys. Res. Lett. **30**(1), 1025 (2003), doi:10.1029/2002GL016413.
13. T. D. Kawahara, C. S. Garnder, and A. Nomura, "Observed temperature structure of the atmosphere above Syowa Station, Antarctica (69°S, 39°E)," J. Geophys. Res. **109**(D12), D12103 (2004), doi:10.1029/2003JD003918.

#138209 - $15.00 USD Received 16 Nov 2010; revised 20 Jan 2011; accepted 30 Jan 2011; published 9 Feb 2011

14. S. E. Palo, J. M. Forbes, X. Zhang, J. M. Russell III, C. J. Mertens, M. G. Mlynczak, G. B. Burns, P. J. Espy, and T. D. Kawahara, "Planetary wave coupling from the stratosphere to the thermosphere during the 2002 Southern Hemisphere pre-stratwarm period," Geophys. Res. Lett. **32**(23), L23809 (2005), doi:10.1029/2005GL024298.
15. C.-Y. She, J. D. Vance, T. D. Kawahara, B. P. Williams, and Q. Wu, "A proposed all-solid-state transportable narrow-band sodium lidar for mesopause region temperature and horizontal wind measurements," Can. J. Phys. **85**(2), 111–118 (2007).
16. J. Yue, C.-Y. She, B. P. Williams, J. D. Vance, P. E. Acott, and T. D. Kawahara, "Continuous-wave sodium D2 resonance radiation generated in single-pass sum-frequency generation with periodically poled lithium niobate," Opt. Lett. **34**(7), 1093–1095 (2009).
17. C.-Y. She, and J. R. Yu, "Doppler-free saturation fluorescence spectroscopy of Na atoms for atmospheric application," Appl. Opt. **34**(6), 1063–1075 (1995).
18. H. Chen, C. Y. She, P. Searcy, and E. Korevaar, "Sodium-vapor dispersive Faraday filter," Opt. Lett. **18**(12), 1019–1021 (1993).

1. Introduction

The mesosphere and lower thermosphere (MLT) region is perhaps the most interesting and least intuitive region in the Earth's atmosphere, e.g., summer is cooler than winter, and large wave activity is caused by atmospheric waves such as gravity waves or tides. In many kinds of ground-based observations, sodium (Na) density lidars have been playing a major role as high temporal/height resolution instruments since ~1980. Subsequent laser development before 1990 improved the 589 nm source to a high spectral resolution (narrowband) light making it possible to measure temperature and wind from backscattered signals tuned to the wavelength in the Doppler broadened/shifted Na D_2 absorption spectrum [1]. The narrowband Na lidar system, however, has not been suitable for deployment in remote sites because the work of maintaining proper operating conditions for three lasers and one pulsed dye amplifier is a complicated task. For worldwide observations, transportable temperature lidars with a solid-state laser are needed. Later the potassium (K) lidar [2, 3] and the iron (Fe) Boltzmann lidar [4] were developed using a tunable alexandrite laser tuned at the potassium (770 nm) or iron (374, 372 nm) resonance lines. However, Na lidars still have a greater advantage because the product of Na atom abundance and backscattering ratio are larger than any other atomic metals in the mesopause region (80-105km) [5]. One of the best solutions for generating a 589 nm resonance light is a Nd:YAG laser. The sum frequency generation (SFG) of a 589 nm coherent light has been demonstrated with two Nd:YAG lasers operating at 1064 and 1319 nm [6, 7]. This technique has already been applied to laser guide star adaptive optics [8], but most lasers are still continuous wave (cw) types and they are untested and require a radically different approach to obtaining altitude and spectral information. In this work, we present a 589 nm pulse lidar based on injection seeded, flash lamp pumped Nd:YAG lasers using the SFG technique. The prominent characteristics of the lidar transmitter include compactness to enable transportability and stable output power with low maintenance. This all-solid state, transportable lidar conducted successful observations at Syowa station in Antarctica (2000-2002) [9] and at Uji in Japan (2007OCT-2009JAN) [10] without any major trouble.

2. Laser system

The schematic layout of the 589 nm coherent light source used in this work is shown in Fig. 1. System parameters of the laser transmitter are summarized in Table 1.

#138209 - $15.00 USD Received 16 Nov 2010; revised 20 Jan 2011; accepted 30 Jan 2011; published 9 Feb 2011

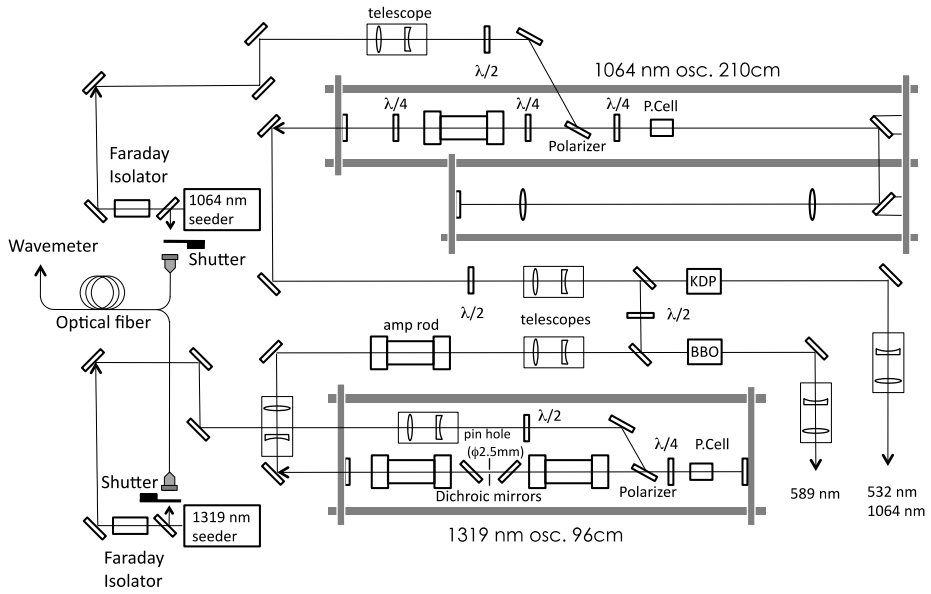

Fig. 1. Schematic of the injection seeded Nd:YAG laser based 589 nm transmitter. Sum frequency generation of 1064 and 1319 nm pulse lasers were applied.

The transmitter is based on two injection–seeded, flashlamp-pumped Nd:YAG lasers (Continuum, Inc., Surelite I-10) with wavelengths of 1064 and 1319 nm. All of the Nd:YAG rods used in this system are 115 mm in length and 6 mm in diameter and anti-reflection coated at each wavelength. For the seeders, we used diode-pumped CW Nd:YAG lasers. The seeders and the pulse lasers are placed on a 1.2 m x 2.4 m optical bench. The 1064 oscillator is a stable resonator using a concave mirror (R = +5 m) and convex Gaussian output coupler. The cavity length is 210 cm. Image relay lenses (f = +400 mm) are placed to make an stable oscillator. The measured temporal pulse width is 23 nsec FWHM and the Q-switch output energy is typically 320 mJ per pulse at 10 Hz repetition rate.

We use a seeder to make the pulse laser single mode, to narrow the spectral linewidth, and to precisely monitor and control the wavelength. The seeder reduces the output pulse energy to 240 mJ. The build-up time difference between the pulses before and after injection seeding is 25 nsec and the time jitter is no more than ± 3 nsec. A piezo controlled mirror optimizes the cavity length for injection seeding by minimizing the pulse build-up time. Sum-frequency mixing uses 150 mJ of laser energy and the rest goes to the KDP crystal to generate a 532 nm source for the Rayleigh lidar observation. The 1319 nm Q-switched oscillator consists of tandem rods in the cavity. The 96-cm cavity consists of a concave rear mirror and a 70% reflectivity flat surface mirror as an output coupler. A pair of intra-cavity dichroic mirrors with long-pass characteristics provides suppression of 1064 nm laser oscillation. The laser energy is typically 55 mJ per pulse, but if injection-seeded, the laser energy drops to 45 mJ per pulse and the pulse builds up 80 nsec earlier. The measured temporal pulse width is 34 nsec FWHM. The output laser diameter is expanded through a telescope from 2.5 mm to 5.0 mm and the laser energy is further amplified up to 100 mJ through an amplification rod.

For frequency mixing, we use a BBO (Beta-Barium Borate) crystal (15 mm x 15 mm x 7 mm) stabilized to a temperature of 40°C. To optimize the sum frequency output, we reduce the beam diameters for the 1064/1319 nm lasers to 3.5/2.5 mm before mixing. A digital delay/pulse generator (Stanford Research Systems Inc., DG535) delayed the 1064 Q-switch trigger timing to synchronize the 1064/1319 nm output and ensure optimum temporal overlap within the BBO. Before reaching the crystal, the polarization of both beams is adjusted using

#138209 - $15.00 USD Received 16 Nov 2010; revised 20 Jan 2011; accepted 30 Jan 2011; published 9 Feb 2011

a λ/2 waveplate for type I phase matching. Input energies of 150/100 mJ at 1064/1319 nm generated 40 mJ of 589 nm laser output with a pulsewidth of as much as 1064 nm. Roughly estimated laser spectral width at 589 nm is 20 MHz FWHM. To certify the laser performance better, chirp measurements is necessary.

Table 1. System parameters for the Na temperature laser transmitter

Pulse Lasers (Continuum, Inc., Surelite I-10)			
	1064 nm	1319 nm	589 nm
Cavity Length (cm)	210	96	-
Pulse Energy (mJ)	150	100	40
Pulsewidth (nsec)	22.6	33.7	22.1
Injection Seeders (Lightwave Inc.)			
	1064 nm	1319 nm	
Model Number	126-1064-100	126-1319-100	
Output Power (mW)	100	100	
Longitudinal mode	single	single	
Line width	< 5 kHz	< 5 kHz	
Polarization	Linear, vertical > 300:1	Linear, vertical > 100:1	

For the lidar observation, fine wavelength tuning of the 589nm laser, i.e., tuning of the 1064/1319 seeders is vital. To monitor the seeder wavelength, we use a wavemeter (Burleigh, WA-1500NIR) with an uncertainty of ± 0.1 pm. The wavelength at 1064/1319 nm is alternately monitored using branched optical fibers and PC-controlled mechanical shutters automatically select the lasers in turn. The total uncertainty of the 589 nm wavelength output is then 0.01 pm (9 MHz) in standard deviation. Fine control of the wavelengths is carried out by tuning the seeder crystal temperature. The seeder wavelength increases linearly with the crystal temperature (e.g., 6.0 x 10^{-3} nm/K for the 1064 seeder) until it reaches a mode hop. The continuous tuning range without mode hop is about 0.06/0.05 nm and the overall tuning range is 0.15/0.17 nm for the 1064/1319 seeders. Consequently, the calculated total tuning range of the mixed frequency is from 589.0946 to 589.1754 nm, sufficiently covering the Na D_2 resonance line at 589.1583 nm (FWHM ~0.002 nm). During observations, the 1319 nm seeder wavelength is fixed at 1319.2012 nm. The 1064 seeder wavelength is alternately tuned between 1064.6221 nm and 1064.6187 nm. The corresponding wavelength shift is between 589.1589 nm (near the D_{2a} peak) and 589.1578 nm (near the minimum between D_{2a} and D_{2b}). The beam divergence is adjusted to < 1 mrad.

3. Lidar observation

The lidar receiver and data processing system are shown in Fig. 2. System parameters for the lidar receiver are shown in Table 2.

#138209 - $15.00 USD Received 16 Nov 2010; revised 20 Jan 2011; accepted 30 Jan 2011; published 9 Feb 2011

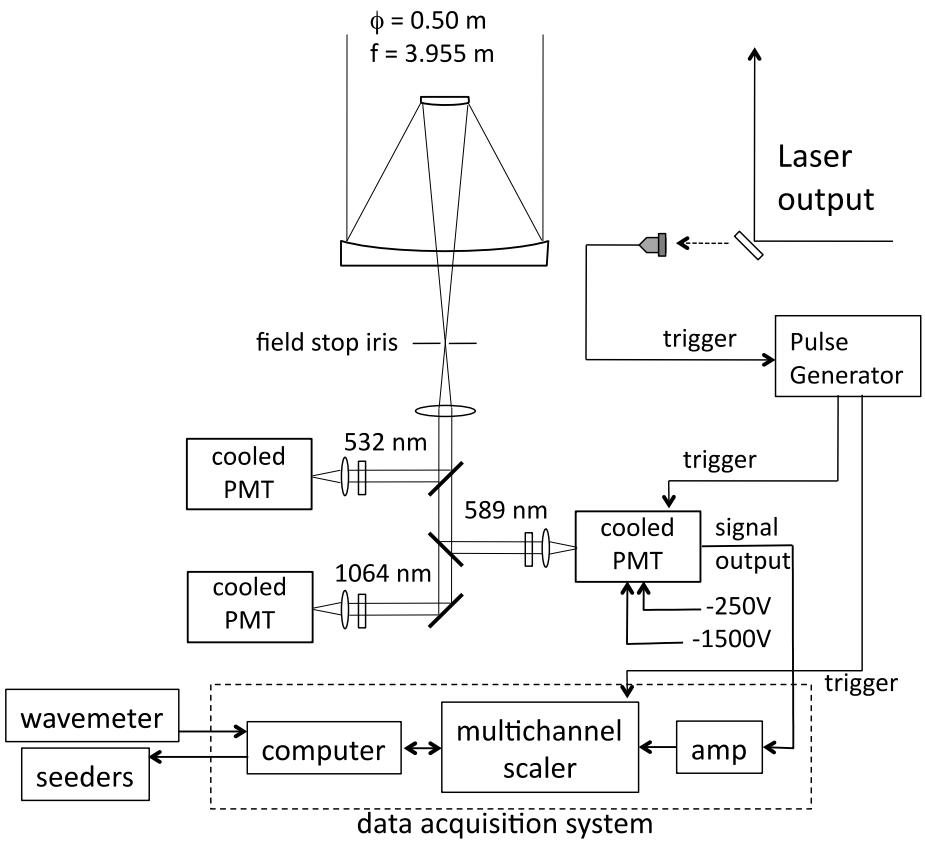

Fig. 2. Schematic of the lidar receiving system.

Table 2. System parameters for the lidar receiver

Telescope	Kiyohara Optics Inc.
Type	Dall-Kirkham Cassegrain
Diameter (m)	0.50
Aperture area (m^2)	0.785
Focal Length (m)	3.995
Interference filter bandpass (nm)	1
Interference filter peak transmission (%)	56
Photo multiplier tube (PMT)	Hamamatsu R943-02
PMT quantum efficiency@589 nm (%)	> 15
Pulse generator	Stanford Research Systems Inc., DG535
Counter	Stanford Research Systems Inc., SR430

The laser is pointed at the zenith direction and the scattered light is collected by a 0.50-m diameter Dall-Kirkham Cassegrain telescope (Kiyohara Optics Inc.) on a pulse-by-pulse basis. The field of view of the telescope is adjustable with a field stop iris (usually set to 2 mrad). The backscattered light is collimated by the lens and the dichroic mirror separates the 589 nm signal to a cooled photomultiplier tube (PMT). The PMT assembly has a gate circuit to switch the high voltage input (–1.5kV) to low voltage input (–250V) and the PMT gate is switched to the lower voltage during the first 90 μsec after the laser shot. A band-pass filter (1 nm FWHM) rejects background light and the backscattered light from the Na layer reaches to a PMT. The signal from the PMT is then amplified and time-series photocounts are counted

#138209 - $15.00 USD Received 16 Nov 2010; revised 20 Jan 2011; accepted 30 Jan 2011; published 9 Feb 2011

by a multichannel scaler. After compiling 1500 laser shots (150 sec observation) at one wavelength, the computer changes the wavelength to another over 30 sec and starts the next measurement.

In order to obtain temperature information from the Doppler-broadened Na spectrum, we adopted the two-frequency technique that was used at Colorado State University and Illinois University [11]. In this simple and reputable technique, the narrowband laser is alternately tuned to the Na D_{2a} peak and the minimum between D_{2a} and D_{2b}. The measured photocounts ratio can be converted to a backscatter cross-section ratio and then finally converted to temperature. System requirements for this measurement are a narrowband laser (< 0.1 pm bandwidth) and fine and accurate wavelength tuning which can be achieved by monitoring and controlling seeder wavelengths. Before routine observations with the two-frequency technique, we confirmed the consistency between the measured wavelength and the Na Doppler spectrum. By shifting the laser wavelength, the Na D_2 spectrum was measured from the backscattered signal intensity from the Na layer. By fitting a theoretical profile, the difference between the measured and the monitored wavelength was found to be less than 0.1 pm (0.1 GHz). This is the same as the wavemeter accuracy.

With this system, the wintertime temperature measurements in the mesopause region (80-115 km) were conducted at Syowa Station (69°S, 39°E) between May 2000 and October 2002 [9]. Figures 3(a) and 3(b) show plots of typical returned signals observed on July 13, 2000, tuned at the D_{2a} peak cross-section and near the minimum between D_{2a} and D_{2b}.

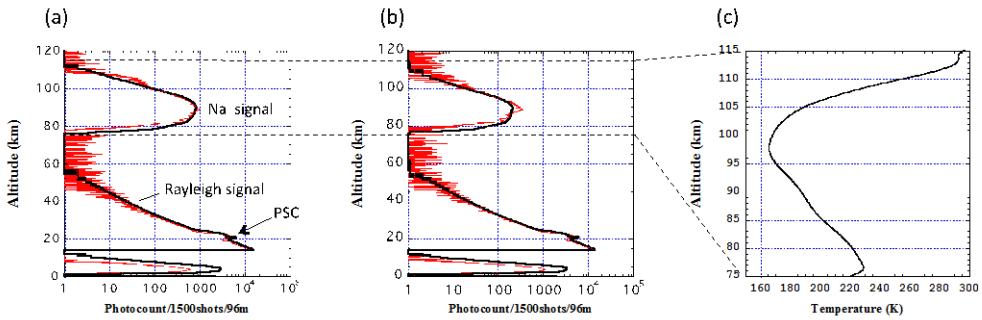

Fig. 3. Received lidar signal tuned at (a) the D_{2a} peak and (b) around the minimum between D_{2a} and D_{2b} (red lines). Thick solid lines in (a) and (b) indicate nightly averaged signals at each wavelength. (c) Nightly averaged temperature structure in the mesopause region.

The red plots indicate integrated the signal of 1500 shots after subtraction of the background signal (5 counts/bin). Thick black solid curves indicate nightly (16 hours) averaged signals at each wavelength on the same day. The height resolution is 96 m. The lower photocounts between ground level and an altitude of 13.5 km is due to low gain PMT operation. Polar stratospheric clouds (PSCs) are typically observed around 23-27 km during the Antarctic winter. Above 60 km, the Rayleigh signal is very weak and instead a strong Na fluorescence is observed between 80 km and 115 km. Figure 3(c) shows the nightly averaged temperature profile between 75 km and 115 km calculated from the nightly averaged Na signals with a vertical resolution of 2.4 km. The mesopause altitude of the day is around 98 km and the temperature is 170 K. Hourly profiles of temperature and Na density are shown in Figs. 4(a) and 4(b), respectively. A downward propagation of the Na peak due to atmospheric tides is seen in Fig. 4(b) as is typical in lidar observations.

#138209 - $15.00 USD Received 16 Nov 2010; revised 20 Jan 2011; accepted 30 Jan 2011; published 9 Feb 2011

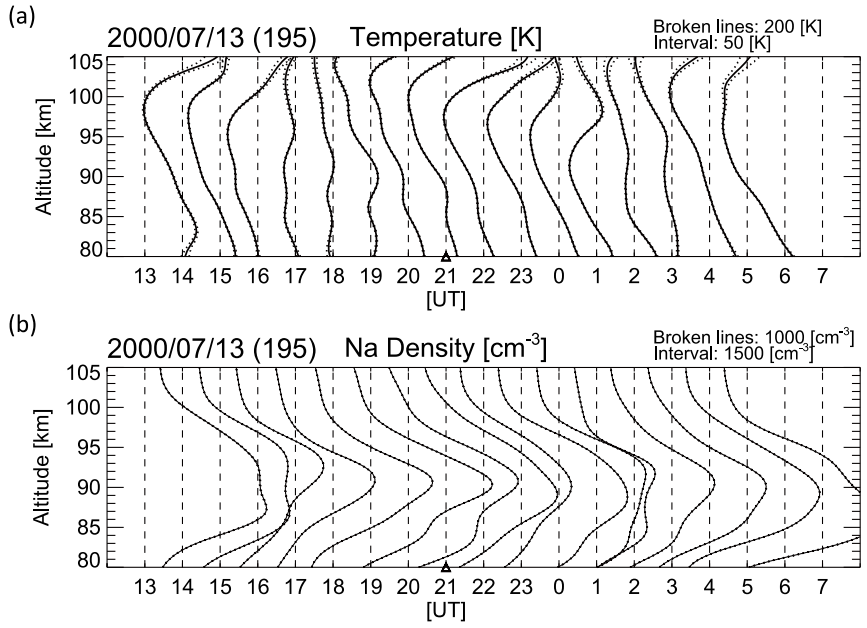

Fig. 4. Hourly profiles of (a) nighttime temperature and (b) sodium density.

Several intercomparison studies were done with the lidar temperature data. The mesopause temperatures (~175 K) in winter months measured at Syowa station by our lidar were about 20 K lower than those observed from a northern hemisphere conjugate site, Andøya (69°N) [9]. The lower winter mesopause temperatures suggested the existence of a hemispheric difference. Hydroxyl rotational nightly-mean temperatures measured at Davis Station (69°S, 78°E) were significantly correlated with Syowa sodium lidar nightly-mean temperatures at 87 km in 2000 (correlation coefficient of 0.68) and 2001 (0.51) despite a site separation of ~1500 km [12]. A comparison with Fe Boltzman lidar measurements at the South Pole (90°S) showed that the annual temperature amplitude at Syowa near 85 km was ~5 K smaller than at the South Pole, which is consistent with the smaller adiabatic heating and cooling expected at lower latitudes [13]. Temperature observations from the SABER instrument on the TIMED spacecraft and from the lidar were used to investigate the nature of planetary wave activity prior to the stratospheric warming in 2002 in the Southern Hemisphere [14].

Lidar observations were done at Uji (35°N, 136°E) in Japan from October 2007 to January 2009 (136 nights). The seasonal and height variations of Na density and temperature in the Northern Hemisphere midlatitude Asian sector were reported for the first time and compared with results obtained in the United States over Colorado (41°N, 105°W) and New Mexico (35°N, 107°W). Winter temperatures at Uji were found to be significantly lower than those at the other two sites [10]. The differences in monthly temperature in winter could be caused by interannual variability of planetary wave activity and of sudden stratospheric warming and/or latitudinal difference in the phase of the nonmigrating tide.

4. Future upgrade

The Na temperature lidar used in our observations in Antarctica and Uji demonstrated high performance and capability without any major operational troubles over several years. A Nd:YAG laser is based on well-established technologies and thus it is currently one of the most reliable and robust lasers. Using the Nd:YAG laser provids a key advantage for the solid

#138209 - $15.00 USD Received 16 Nov 2010; revised 20 Jan 2011; accepted 30 Jan 2011; published 9 Feb 2011

state Na systems compared with other solid state lidars. Combining the solid state Na system with the established narrowband lidar techniques has potential to be upgraded to a robust wind and temperature lidar [15]. For the wind measurement, our Na lidar needs (1) more precise 589 nm laser frequency monitoring (including chirp) and locking and (2) tuning to three different frequencies for the measurement of Doppler shifted Na spectrum.

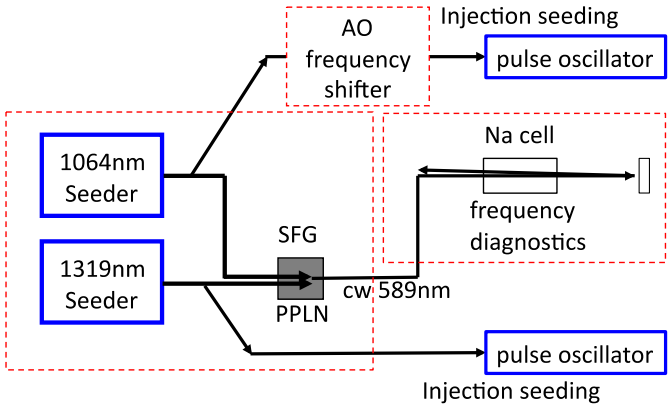

Fig. 5. Schematic of the proposed injection seeding part including the SFG system using high power seeders, Doppler free saturation spectroscopy with a Na cell and an AO frequency shifter.

Figure 5 shows the schematic of the injection seeding system for precise laser frequency diagnostics using a Na vapor cell with a frequency shifter using acousto-optic (AO) crystals. High power 1064/1319 nm seeders with a Periodically Poled Lithium Niobate (PPLN) crystal demonstrated the generation of narrowband cw 589 nm light by a single-pass SFG [16]. The narrowband cw 589 nm light source enables us to measure the fine structure of Doppler free fluorescence spectra from the heated Na cell and to lock the laser frequency at the D_{2a} Lamb dip (ν_0) with an accuracy of a few MHz [17]. An acousto-optic frequency shifter (AOFS) can precisely shift the laser frequency up ($+\Delta\nu$) and down ($-\Delta\nu$) from ν_0 in less than 1 microsecond. The use of AOFS in the middle of the 1064 seeding line results in cyclical operation of the 589 nm emission at ν_0 and $\nu_0 \pm \Delta\nu$, so that we can measure the temperature and wind from the measured Doppler broadened and shifted Na absorption spectrum. In addition, a Faraday dispersive filter used as an ultra narrowband optical filter at the Na D_2 spectrum in the receiving system enables us to reject the background signal from the Sun and to do daytime measurements [18]. Note that all these techniques have been tested in actual lidar operation and proven robust. The proper combination of these mature technologies will lead to a new all solid-state and transportable Na wind/temperature lidar on a 24 h basis.

5. Summary and conclusion

We built an all solid-state Na lidar and conducted long-term observations in Antarctica and Japan for several years. The characteristics of the lidar transmitter are summarized below.

1. The transmitter is based on Nd:YAG laser technology which is one of the most stable and reliable, and thus robust.
2. The SFG technique with a BBO crystal is used to generate 589 nm coherent light from the pulse lasers at 1064 and 1319 nm.
3. Mesopause temperatures were measured using the narrowband 589 nm light resulted from injection seeding technique with fine wavelength monitoring by a wavemeter.

#138209 - $15.00 USD Received 16 Nov 2010; revised 20 Jan 2011; accepted 30 Jan 2011; published 9 Feb 2011

4. The long-term lidar observation without any major trouble demonstrated high performance and capability.

The lidar can be upgraded to a robust transportable wind/temperature lidar and will allow us 24 hour continuous observation.

Acknowledgements

The lidar observation in Antarctica was supported by the 40^{th}-42^{nd} Japanese Antarctic Research Expedition. The authors also wish to thank Continuum, Inc. and Excel Technology Japan K.K. for the construction of the laser.

#138209 - $15.00 USD Received 16 Nov 2010; revised 20 Jan 2011; accepted 30 Jan 2011; published 9 Feb 2011